

# Generalized Additive Models for Pair-Copula Constructions

Thibault Vatter\*

Institute of Mathematics,  
École Polytechnique Fédérale de Lausanne,  
Lausanne, Switzerland

and

Thomas Nagler†

Lehrstuhl für Mathematische Statistik,  
Technische Universität München,  
Munich, Germany

December 9, 2024

## Abstract

Pair-copula constructions are flexible models for the dependence in a random vector that have attracted a lot of interest in recent years. In this paper, we use generalized additive models to extend pair-copula constructions to allow for effects of covariates on the dependence parameters. We let each pair-copula parameter depend directly on the covariates in a parametric, semi-parametric or non-parametric way. We propose a sequential estimation method that we study by simulation, and apply our method to investigate the time-varying dependence structure between the intraday returns on four major foreign exchange rates.

*Keywords:* Conditional copula, covariates, dependence modeling, partially linear models, semiparametric, smoothing and nonparametric regression

---

\*Thibault Vatter is Postdoctoral researcher, École Polytechnique Fédérale de Lausanne, EPFL-SB-MATHAA-STAT, Station 8, CH-1015 Lausanne, Switzerland (email: thibault.vatter@epfl.ch)

†Thomas Nagler is PhD candidate, Lehrstuhl für Mathematische Statistik, Technische Universität München, Boltzmannstraße 3, 85748 Garching b. München, Germany (email: thomas.nagler@tum.de)

# 1 INTRODUCTION

*Pair-copula constructions* (PCCs) are flexible representations of the dependence underlying a multivariate distribution. Popularized in [Aas et al. \(2009\)](#), they have become a hot topic of multivariate analysis over the last couple of years. The idea is to model the joint distribution of a  $d$ -dimensional random vector by considering pairs of conditional random variables. Let us consider a three dimensional example. The joint density  $f_{1,2,3}(\mathbf{x})$ ,  $\mathbf{x} \in \mathbb{R}^3$ , of a vector of continuous random variables  $\mathbf{X} = (X_1, X_2, X_3)$  can be decomposed as

$$f_{1,2,3}(\mathbf{x}) = f_1(x_1) \times f_2(x_2) \times f_3(x_3) \times c_{1,2} \{F_1(x_1), F_2(x_2)\} \times c_{2,3} \{F_2(x_2), F_3(x_3)\} \\ \times c_{1,3;2} \{F_{1|2}(x_1 | x_2), F_{3|2}(x_3 | x_2); x_2\},$$

where

- $f_1, f_2, f_3$  (and  $F_1, F_2, F_3$ ) are the marginal densities (and distributions),
- $c_{1,2}$  is the joint density of  $F_1(X_1)$  and  $F_2(X_2)$ ,
- $c_{2,3}$  is the joint density of  $F_2(X_2)$  and  $F_3(X_3)$ ,
- $c_{1,3;2}$  is the joint density of  $F_{1|2}(X_1 | X_2)$  and  $F_{3|2}(X_3 | X_2)$  conditional on  $X_2 = x_2$ .

The above decomposition can be generalized to an arbitrary dimension  $d$  and leads to tractable and very flexible models.

In general, the conditional density  $c_{1,3;2}$  is also a function of  $x_2$ . However, this effect is often ignored for the sake of tractability, in which case we speak about a simplified PCC. When this so-called *simplifying assumption* is made, the complete joint distribution can be built using unconditional bivariate copulas. Discussions on the simplifying assumption can be found in [Haff et al. \(2010\)](#), [Stöber et al. \(2013\)](#), and [Spanhel & Kurz \(2015\)](#).

An natural extension of PCCs includes the effect of covariates. This is particularly useful when one wants to investigate the influence of exogenous variables (such as space or time) on a complex dependence structure. For instance, the joint spatio-temporal modeling of several hydrograph flood variables, such as the flood peak, the hydrograph volume and hydrograph duration, is necessary to design and manage risks for hydraulic structures like dams ([Requena et al. 2013](#)). Another example is the modeling of the joint distribution of intraday returns on exchange rates, whose the dependence structure changes over time due to the cyclical nature of market activity. Even when the covariate is random, we are often only willing to study its effect on the joint distribution of a response vector of interest. In this case, it is usually unnecessary or inconvenient to model its stochastic behavior explicitly, and a regression-like theory for PCCs is required. In the hydrological example above, when a region under study characterized by large hydro-climatic heterogeneities, the inclusion of additional (potentially random) descriptors in the model is important; especially as the ultimate goal is the extrapolation (prediction) at ungauged sites. Similarly, scheduled economic news, such as the monthly release of the US unemployment rate, or the Federal Open Market Committee (FOMC) press conference, impact in a crucial way the dependence structure between intraday returns. Previous work in this direction includes

regime switching PCC (Stöber & Czado 2014), and spatial PCC models (Gräler 2014, Erhardt et al. 2015a,b), where the individual parameters of the pair-copulas were modeled as linear functions of distances between different locations.

To relax the simplifying assumption and model the influence of covariates, the appropriate statistical tool is the *conditional copula*. This made its first appearance in the seminal work of Patton (2002) in a time-series context. While Patton’s approach is parametric, a fully nonparametric alternative was later proposed by Gijbels et al. (2011) and Veraverbeke et al. (2011). Acar et al. (2011) discuss a semiparametric model where the dependence parameter is modeled as a smooth nonparametric function of a covariate, which is estimated by a kernel-based local likelihood approach. This methodology was used by Acar et al. (2012) for the estimation of the conditional dependence in a three-dimensional PCC. A Bayesian method was proposed by Craiu & Sabeti (2012) and extended by Sabeti et al. (2014) to allow for multiple covariates.

Recently, Vatter & Chavez-Demoulin (2015) proposed an alternative approach based on generalized additive models (GAMs, see Hastie & Tibshirani 1990, Green & Silverman 2000) and spline smoothing. Building on the flexibility of GAMs, the copula parameter is modeled as a parametric, semiparametric or non-parametric function of the covariates. As the estimation is based on maximizing a penalized likelihood, the method is stable and fast, even for large datasets.

In this paper, we utilize Vatter & Chavez-Demoulin (2015)’s GAMs for including the effects of covariates on a PCC. The structure of the paper is as follows. In Section 2, we first introduce PCCs and the GAM framework of Vatter & Chavez-Demoulin (2015). Then, we discuss inference issues related to PCCs with covariates. We study the estimator’s behavior by simulation in Section 3. In Section 4, we model the time-varying dependence structure between the intraday returns on four major foreign exchange rates. We conclude with a discussion in Section 5.

## 2 METHODOLOGY

### 2.1 Pair-Copula Constructions

Let  $\mathbf{X} = (X_1, \dots, X_d) \sim F$  be a  $d$ -variate random vector. By the theorem of Sklar (1959), any  $F$  can be represented by its marginal distributions  $F_1, \dots, F_d$  and a *copula*  $C$ , such that

$$F(x_1, \dots, x_d) = C\{F_1(x_1), \dots, F_d(x_d)\}. \quad (1)$$

The copula  $C$  describes the dependence structure of  $\mathbf{X}$  and is the joint distribution of the random vector  $\mathbf{U} = (U_1, \dots, U_d) = (F_1(X_1), \dots, F_d(X_d))$ . Conversely, if  $C$  is a  $d$ -dimensional copula and  $F_1, \dots, F_d$  are univariate distributions, then the right-hand side of Equation (1) defines a valid multivariate distributions with fixed margins. Furthermore, if

$F$  has a density, we can differentiate both sides of [Equation \(1\)](#) to get

$$f(x_1, \dots, x_d) = c\{F_1(x_1), \dots, F_d(x_d)\} \times \prod_{k=1}^d f_k(x_k),$$

where  $f, c, f_1, \dots, f_d$  are the densities corresponding to  $F, C, F_1, \dots, F_d$  respectively.

In this context, a pair-copula construction is a graphical model for the copula density  $c$ . Following [Joe \(1997\)](#) and [Bedford & Cooke \(2001, 2002\)](#), any  $c$  can be decomposed into a product of  $d(d-1)/2$  bivariate (conditional) copula densities. The decomposition is not unique, but all possible decompositions can be organized as graphical structure, called *regular vine (R-vine)* - a sequence of trees  $T_m = (V_m, E_m)$  ( $m = 1, \dots, d-1$ ) satisfying the following conditions:

1.  $T_1$  is a tree with nodes  $V_1 = \{1, \dots, d\}$  and edges  $E_1$ .
2. For  $m \geq 2$ ,  $T_m$  is a tree with nodes  $V_m = E_{m-1}$  and edges  $E_m$ .
3. (*Proximity condition*) Whenever two nodes in  $T_{m+1}$  are joined by an edge, the corresponding edges in  $T_m$  must share a common node.

The corresponding tree sequence is also called the *structure* of the PCC. A PCC identifies each edge  $e$  of the trees with a bivariate copula  $c_{j_e, k_e; D_e}$  (a so-called *pair-copula*). The joint density of the PCC can then be written as the product of all pair-copula densities:

$$c(\mathbf{u}) = \prod_{m=1}^{d-1} \prod_{e \in E_m} c_{j_e, k_e; D_e} \{C_{j_e|D_e}(u_{j_e} | \mathbf{u}_{D_e}), C_{k_e|D_e}(u_{k_e} | \mathbf{u}_{D_e}); \mathbf{u}_{D_e}\}, \quad (2)$$

where  $\mathbf{u}_{D_e} := (u_\ell)_{\ell \in D_e}$  is a subvector of  $\mathbf{u} = (u_1, \dots, u_d) \in [0, 1]^d$  and  $C_{j_e|D_e}$  is the conditional distribution of  $U_{j_e} | \mathbf{U}_{D_e}$ . The set  $D_e$  is called the *conditioning set* and the indices  $j_e, k_e$  form the *conditioned set*. Put differently, the pair-copula density  $c_{j_e, k_e; D_e}$  describes the dependence between the two variables  $U_{j_e}$  and  $U_{k_e}$ , conditional on  $\mathbf{U}_{D_e}$ . The conditioning set grows with the tree level: for  $e \in E_m$ , the conditioning vector has  $m-1$  components, for  $e \in E_{m+1}$ ,  $m$  components, etc.

**Example 1.** *The density of a PCC corresponding to the tree sequence in [Figure 1](#) is*

$$\begin{aligned} c(u_1, \dots, u_5) &= c_{1,2}(u_1, u_2) \times c_{1,3}(u_1, u_3) \times c_{3,4}(u_3, u_4) \times c_{3,5}(u_3, u_5) \\ &\quad \times c_{2,3;1}(u_{2|1}, u_{3|1}; u_1) \times c_{1,4;3}(u_{1|3}, u_{4|3}; u_3) \times c_{1,5;3}(u_{1|3}, u_{5|3}; u_3) \\ &\quad \times c_{2,4;1,3}(u_{2|1,3}, u_{4|1,3}; \mathbf{u}_{\{1,3\}}) \times c_{4,5;1,3}(u_{4|1,3}, u_{5|1,3}; \mathbf{u}_{\{1,3\}}) \\ &\quad \times c_{2,5;1,3,4}(u_{2|1,3,4}, u_{5|1,3,4}; \mathbf{u}_{\{1,3,4\}}), \end{aligned}$$

where we use the notation  $u_{j_e|D_e} := C_{j_e|D_e}(u_{j_e} | \mathbf{u}_{D_e})$ .

In a simplified PCC, we ignore the influence of  $\mathbf{u}_{D_e}$  on the pair-copula density  $c_{j_e, k_e; D_e}$ .

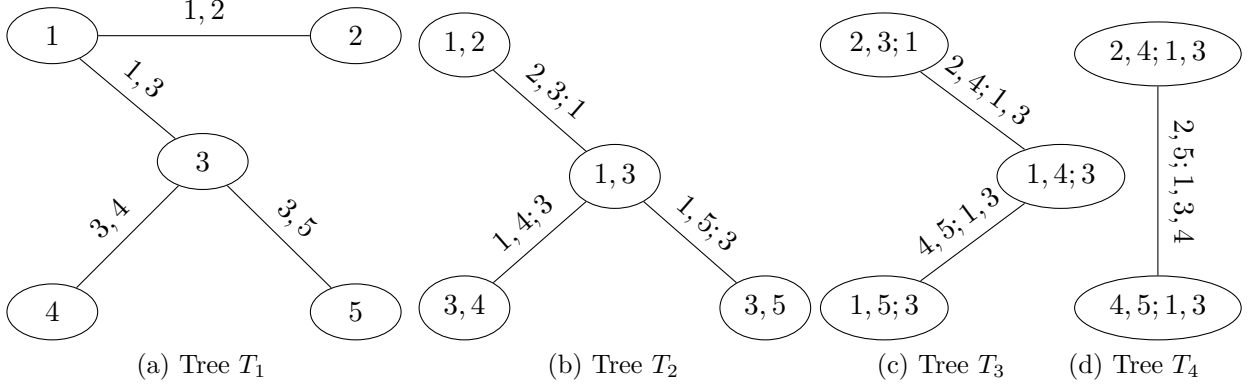


Figure 1: Example of a Regular Vine Tree Sequence. The numbers represent the variables,  $x, y$  denote the bivariate distribution of  $x$  and  $y$ , and  $x, y; z$  denote the bivariate distribution of  $x$  and  $y$  conditional on  $z$ . Each edge corresponds to a bivariate pair-copula in the PCC.

Thus, the density collapses to

$$c(\mathbf{u}) = \prod_{m=1}^{d-1} \prod_{e \in E_m} c_{j_e, k_e; D_e} \{C_{j_e|D_e}(u_{j_e} | \mathbf{u}_{D_e}), C_{k_e|D_e}(u_{k_e} | \mathbf{u}_{D_e})\}. \quad (3)$$

However, since each pair-copula can be modeled separately, simplified PCCs are highly flexible. Furthermore, they can easily be interpreted, as each pair-copula describes the dependence for a specific (conditional) bivariate random vector. For a more extensive treatment, we refer to [Aas et al. \(2009\)](#) and [Czado \(2010\)](#).

## 2.2 Generalized Additive Models for Pair-Copula Constructions

To both relax the simplifying assumption and include a vector  $\mathbf{w}$  of exogenous covariates, we need to model the conditional copula density for each edge of the PCC explicitly. The joint density can thus be rewritten

$$c(\mathbf{u}; \mathbf{w}) = \prod_{m=1}^{d-1} \prod_{e \in E_m} c_{j_e, k_e; D_e} \{C_{j_e|D_e}(u_{j_e} | \mathbf{u}_{D_e}), C_{k_e|D_e}(u_{k_e} | \mathbf{u}_{D_e}); \mathbf{w}_e\}, \quad (4)$$

where  $\mathbf{w}_e = (\mathbf{w}, \mathbf{u}_{D_e})$  contains both the exogenous covariates and the variables in the conditioning set. Note that  $\mathbf{w}_e = \mathbf{w}$  for  $e \in E_1$ . Furthermore, if  $\mathbf{w}_e = \mathbf{u}_{D_e}$  for each  $e \in E_m$  ( $m = 1, \dots, d-1$ ), we have the non-simplified PCC from [Equation \(2\)](#) with no exogenous covariates. Because, to the best of our knowledge, the only dataset known to violate the simplifying assumption was studied by [Acar et al. \(2012\)](#), the usefulness of non-simplified PCCs has yet to be established. Thus, while emphasizing that they can be handled by our methodology, we will not pursue this path any further in this paper.

An important subclass of [Equation \(4\)](#), and the focus of the remainder of this paper, is obtained by writing  $\mathbf{w}_e = \mathbf{w}$  for each  $e \in E_m$ ,  $m = 1, \dots, d-1$ . In this case, the simplifying

assumption is satisfied, but the effects of  $\mathbf{w}$  are still included, and we call this model a *simplified PCC with exogenous covariates*.

To make this construction practically useful, one assumes a parametric form for the (conditional) copula density  $c_e\{\cdot, \cdot; \eta_e(\mathbf{w})\}$ . For common copula families, there is a one-to-one mapping between the copula parameter  $\eta_e$  and Kendall's  $\tau_e$ , a copula-based measure of concordance (see, e.g., [Nelsen 2006](#), Section 5.1.1). For simplicity, we assume throughout that such a relationship exists. When this is not the case (or for multi-parameter families), the methodology can still be applied to the copula parameter (or to one of them). See [Vatter & Chavez-Demoulin \(2015\)](#) for an additional discussion.

We can then reparameterize the conditional copula as a function of its corresponding Kendall's  $\tau$ , and we write  $c_e(\cdot, \cdot; \tau_e(\mathbf{w}))$ . Dropping the subscript  $e$  for clarity, [Vatter & Chavez-Demoulin \(2015\)](#) proposed to model the variation of the dependence parameter with respect to the covariates as

$$\tau(\mathbf{w}; \boldsymbol{\theta}) = g \left\{ \mathbf{z}^\top \boldsymbol{\beta} + \sum_{k=1}^K s_k(\mathbf{t}_k) \right\}, \quad (5)$$

where

- $g(x) = (e^x - 1)/(e^x + 1)$  is a link between the GAM and Kendall's  $\tau$ ,
- $\mathbf{z}$  and  $\mathbf{t}_k$  are subsets of  $\mathbf{w}$  or products thereof (to allow interactions),
- $\boldsymbol{\beta} \in \mathbb{R}^P$  is a vector of parameters,
- $s_k : \mathbb{S}_k \rightarrow \mathbb{R}$  are smooth functions supported on closed interval  $\mathbb{S}_k \subset \mathbb{R}$  for all  $k$ ,
- $\boldsymbol{\theta}$  is the vector of stacked parameters, containing both  $\boldsymbol{\beta}$  and  $s_k$  for all  $k$ .

Models of this form are also called *partially linear models* ([Härdle & Liang 2007](#)): they consist of a linear component,  $\mathbf{z}^\top \boldsymbol{\beta}$ , and a nonlinear component,  $\sum_{k=1}^K s_k(\mathbf{t}_k)$ .

For instance, consider the three dimensional PCC from [Figure 2](#) is simplified, and assume that each pair-copula depends on a covariate  $x$  and on time  $t$ . As such, the vector of covariates  $\mathbf{w} = (x, t)$  is the same in tree  $T_1$  and tree  $T_2$ . Supposing that we want to allow for a nonlinear effect of time-variation and assume the effect of the other covariate to be linear, a model for the corresponding conditional pair-copulas can be written as

$$\begin{aligned} \tau_{1,2}(\mathbf{w}) &= g \{x\beta_{1,2} + s_{1,2}(t)\}, \\ \tau_{1,3}(\mathbf{w}) &= g \{x\beta_{1,3} + s_{1,3}(t)\}, \\ \tau_{2,3;1}(\mathbf{w}) &= g \{x\beta_{2,3;1} + s_{2,3;1}(t)\}. \end{aligned}$$

In the non-simplified case, the covariate vector for the third pair-copula would be augmented such that  $\mathbf{w}_{2,3;1} = (\mathbf{w}, u_1)$ .

In this paper, we assume that all smooth functions  $s_k$  are twice continuously differentiable on their support  $\mathbb{S}_k$ , and admit a finite-dimensional basis-quadratic penalty representation (cf. [Wood 2006](#)). In particular, we focus on *natural cubic splines* (NCSs). A NCS  $s : \mathbb{S} \rightarrow \mathbb{R}$



Figure 2: A Three-Dimensional Regular Vine Tree Sequence. The numbers represent the variables,  $x, y$  denote the bivariate distribution of  $x$  and  $y$ , and  $x, y, z$  denote the bivariate distribution of  $x$  and  $y$  conditional on  $z$ . Each edge corresponds to a bivariate pair-copula in the PCC.

is defined with a fixed sequence of  $m$  knots,  $\inf \mathbb{S} = y_0 < y_1 < \dots < y_m < y_{m+1} = \sup \mathbb{S}$ . It is linear on the two extreme intervals  $[y_0, y_1]$  and  $[y_m, y_{m+1}]$  and twice continuously differentiable on  $\mathbb{S}$ . As such, it can be parametrized using  $\mathbf{s} \in \mathbb{R}^m$ , and there exists a unique  $m \times m$  symmetric matrix  $\mathbf{S}$  of rank  $m - 2$  such that  $\int_{\mathbb{S}} s''(t)^2 dt = \mathbf{s}^\top \mathbf{S} \mathbf{s}$ . This matrix is fixed in the sense that it depends on the knots but not on  $\mathbf{s}$ .

Let  $m_k$  denote the basis size of  $s_k$ ; then  $\boldsymbol{\theta} \in \Theta \subseteq \mathbb{R}^l$ , where  $p = P + \sum_{k=1}^K m_k$ . For  $\mathbf{u} \in [0, 1]^2$  and  $\boldsymbol{\theta} \in \Theta$ , we denote the log-likelihood function conditional on  $\mathbf{w}$  by  $\ell(\mathbf{u}, \mathbf{w}; \boldsymbol{\theta}) = \log c\{\mathbf{u}; \tau(\mathbf{w}; \boldsymbol{\theta})\}$ , assuming that the dependence parameter is sufficient to identify the copula. Then, considering a random sample of  $n$  observations  $\{\mathbf{u}^j, \mathbf{w}^j\}_{j=1}^n$ , the log-likelihood is  $\ell(\boldsymbol{\theta}) = n^{-1} \sum_{j=1}^n \ell(\mathbf{u}^j, \mathbf{w}^j; \boldsymbol{\theta})$ . Because, for arbitrarily chosen basis sizes, its maximizer is unlikely to yield smooth estimates of  $s_1, \dots, s_K$ , we add roughness penalties to each nonparametric component, and define the penalized log-likelihood

$$\ell(\boldsymbol{\theta}, \boldsymbol{\gamma}) = \ell(\boldsymbol{\theta}) - \frac{1}{2} \sum_{k=1}^K \gamma_k \int_{\mathbb{S}_k} s_k''(\mathbf{t}_k)^2 d\mathbf{t}_k = \ell(\boldsymbol{\theta}) - \frac{1}{2} \boldsymbol{\theta}^\top \mathbf{p}(\boldsymbol{\gamma}) \boldsymbol{\theta}, \quad (6)$$

with  $\boldsymbol{\gamma} \in (\mathbb{R}_+ \cup \{0\})^K$ , a vector of smoothing parameters, and  $\mathbf{p}(\boldsymbol{\gamma})$  is a  $p \times p$  block diagonal matrix with  $K + 1$  blocks; the first  $P \times P$  block is filled with zeros and the remaining  $K$  are equal to  $\gamma_k \mathbf{S}_k$ , where  $\mathbf{S}_k$  is the quadratic penalty representation of  $s_k$ . We define the penalized maximum log-likelihood estimator as

$$\hat{\boldsymbol{\theta}} = \underset{\boldsymbol{\theta} \in \Theta}{\operatorname{argmax}} \ell(\boldsymbol{\theta}, \boldsymbol{\gamma}). \quad (7)$$

In [Vatter & Chavez-Demoulin \(2015\)](#), it is shown that one step of Fisher's scoring algorithm can be approximated by a generalized ridge regression. In other words,  $\hat{\boldsymbol{\theta}}$  is found iteratively by solving

$$\boldsymbol{\theta}^{[l+1]}(\boldsymbol{\gamma}) = \underset{\boldsymbol{\theta} \in \Theta}{\operatorname{argmin}} \left\{ \|\mathbf{y}^{[l]} - \mathbf{d}^{[l]} \boldsymbol{\theta}\|_{\mathbf{a}^{[l]}}^2 + \|\boldsymbol{\theta}\|_{\mathbf{p}(\boldsymbol{\gamma})}^2 \right\}, \quad (8)$$

where  $\|\mathbf{x}\|_{\mathbf{w}}^2 = \mathbf{x}^\top \mathbf{w} \mathbf{x}$  and  $\mathbf{y}^{[l]}$ ,  $\mathbf{d}^{[l]}$  and  $\mathbf{a}^{[l]}$  depend only on the data,  $\boldsymbol{\theta}^{[l]}$  and the copula family. With  $\mathbf{s}^{[l]}(\boldsymbol{\gamma})$  the so-called influence or hat matrix at the  $l$ th iteration, defined such that  $\mathbf{s}^{[l]}(\boldsymbol{\gamma}) \mathbf{y}^{[l]} = \mathbf{d}^{[l]} \boldsymbol{\theta}^{[l+1]}(\boldsymbol{\gamma})$ , we can now define the *effective or equivalent degrees of freedom*

(EDF) at the  $l$ th iteration as

$$\text{EDF}^{[l]}(\boldsymbol{\gamma}) = \text{tr} \{ \mathbf{s}^{[l]}(\boldsymbol{\gamma}) \} .$$

For additional discussions and alternative definitions of the EDF in the context of exponential families, see [Hastie & Tibshirani \(1990\)](#) or [Green & Silverman \(2000\)](#). To balance goodness-of-fit and dimensionality, [Vatter & Chavez-Demoulin \(2015\)](#) minimize the *generalized cross-validation* sum of squares ([Craven & Wahba 1979](#))

$$\text{GCV}^{[l]}(\boldsymbol{\gamma}) = \frac{n^{-1} \|\mathbf{y}^{[l]} - \mathbf{s}^{[l]}(\boldsymbol{\gamma})\mathbf{y}^{[l]}\|^2_{\mathbf{a}^{[l]}}}{\left\{ 1 - n^{-1} \text{EDF}^{[l]}(\boldsymbol{\gamma}) \right\}^2}$$

at each generalized ridge iteration, and a model’s EDF is the final  $\text{EDF}^{[l]}(\boldsymbol{\gamma})$ , obtained at convergence.

### 2.3 Generalized Additive Model Selection for a Single Family

At this step, the goal is to select a GAM assuming a known pair-copula family. Generally speaking, there can be at most one unique smooth function  $s_{e,k}$  for each covariate. But usually there is no prior knowledge of its shape. This raises two questions:

1. Which of the covariates have an influence?
2. What is the appropriate basis size for each of the smooth functions?

Below, we give heuristically motivated answers to these questions, and we summarize this method in [Algorithm 1](#) (in the appendix).

To answer the **first question**, we first set the basis size for each component to ten (i.e.  $m_k = 10$  for each  $k$ ), which is at the same time big enough to detect obvious non-linear relations and small enough to be quickly estimated. Second, we use a variant of backward elimination, where we start with all the covariates, remove at each step the ones whose individual  $p$ -values are above a pre-specified level  $\alpha$ , re-estimate the model and iterate until all remaining covariates are significantly non-zero.

In addition to the usual issues related to step-wise selection methods,  $p$ -values for the smooth terms are necessarily approximate. As suggested in [Marra & Wood \(2012\)](#) and [Wood \(2013b,a\)](#) in the exponential family context, we compute individual  $p$ -values using a Wald test. To compute the test statistics, we use a covariance matrix that results from the Bayesian interpretation of GAMs. While there is no optimality result for the power, [Marra & Wood \(2012\)](#), extending the analysis of [Nychka \(1988\)](#), motivated the use of this covariance matrix by showing that the resulting intervals have better frequentist performance (power and size under the null) than those computed using a strictly frequentist approximation.

As for the **second question**, once the set of covariates is selected, the basis size of the GAM’s smooth components is usually not critical. On the one hand, it should be large enough so that the underlying features in the data can be well approximated. On the other hand, it should be small enough to maintain good computational efficiency and low variance

(although partially addressed by the penalization). To achieve this trade-off, we do the following, with  $J$  the set of selected covariates:

1. Start with a small basis size ( $b_j = 10$  for  $j \in J$ ).
2. Fit the GAM.
3. Check which of the estimated EDFs are “close” to the upper limit. If this is the case, namely if  $\text{EDF}_j > 0.8 \times b_j$  for any  $j \in J$ , increase the corresponding  $b_j$ .
4. Iterate 2. and 3. until no further increase is required for any of  $j \in J$ .

Additionally, at each step, we make sure that no individual basis size is greater than the sample size divided by thirty. While not theoretically justified, keeping a reasonably large ratio of number of observations to number of parameters is a rule of thumb that is useful in this context. The reason is that we frequently observe numerical instabilities when this ratio is around thirty and lower.

## 2.4 Sequential Estimation of a Pair-Copula Construction

To estimate PCCs, it is common to follow a sequential approach (see e.g. [Aas et al. 2009](#), [Hobæk Haff 2013](#), [Nagler & Czado 2016](#)), which we outline below. Assume that  $\mathbf{u}^i = (u_1^i, \dots, u_d^i)$  ( $i = 1, \dots, n$ ) are observations from a pair-copula construction and the vine structure is known. Then, the pair-copulas of the first tree,  $T_1$ , can be easily estimated using the method described in the previous subsection. This is not as straightforward for trees  $T_m$  with  $m \geq 2$  since data from the densities  $c_{j_e, k_e; D_e}$  are unobserved. However, we can sequentially construct pseudo-observations by an appropriate transformation of the data.

Define the  $h$ -functions (cf. [Aas et al. 2009](#)) corresponding to a pair-copula density  $c_{j_e, k_e; D_e}(u, v; \cdot)$  as

$$h_{j_e|k_e; D_e}(u | v; \cdot) = \int_0^u c_{j_e, k_e; D_e}(s, v; \cdot) ds, \quad h_{k_e|j_e; D_e}(u | v; \cdot) = \int_0^v c_{j_e, k_e; D_e}(u, s; \cdot) ds,$$

for all  $(u, v) \in [0, 1]^2$ . The dot in the third argument represents one of the GAM-formulations in [Section 2.2](#). A crucial insight is the following: Assume we have (pseudo-)observations from the pair-copula density  $c_{j_e, k_e; D_e}$ , denoted as  $(u_{j_e|D_e}^i, u_{k_e|D_e}^i)$  ( $i = 1, \dots, n$ ). Then we can construct pseudo-observations for the next tree by setting

$$u_{j_e|D_e \cup k_e}^i = h_{j_e|k_e; D_e}(u_{j_e|D_e}^i | u_{k_e|D_e}^i; \cdot), \quad u_{k_e|D_e \cup j_e}^i = h_{k_e|j_e; D_e}(u_{k_e|D_e}^i | u_{j_e|D_e}^i; \cdot), \quad i = 1, \dots, n. \quad (9)$$

As only the estimates of each pair-copula in  $T_l$  are required to compute pseudo-observations for tree  $T_{l+1}$ , we make use of the following sequential estimation and model selection procedure, starting with tree  $T_1$ :

1. For each edge in the tree:
  - (a) Select the covariates and estimate a GAM for each copula family via [Section 2.3](#).

- (b) Use the AIC to choose a copula family.
- (c) Use the estimates to construct pseudo-observations for the next tree via (9).

2. Go to the next tree.

The fact that the tree sequence  $T_1, T_2, \dots$ , is a regular vine guarantees that at any step in this procedure, all required pseudo-observations are available.

## 3 SIMULATIONS

### 3.1 Setup

We consider a simplified GAM-PCC in five dimensions using the vine structure depicted in Figure 1. The Kendall's  $\tau$  of each pair-copula is set as the partially linear model

$$\tau_e(\mathbf{z}, t) = g \{ \mathbf{z}^\top \boldsymbol{\beta} + s_{e,r}(t) \}. \quad (10)$$

The covariate vector  $\mathbf{z} \in \mathbb{R}^{10}$  consists of five Bernoulli(0.5) variables and five standard normal variables (in that order). The covariate  $t$  is a deterministic sequence ranging from 0 to 1 in equidistant steps. In total there are eleven covariates. We set

$$\boldsymbol{\beta} = 0.3 \times (1, 1, -1, 0, 0, -1, -1, -1, 0, 0)^\top,$$

so that only six components of  $\mathbf{z}$  actually have an influence on  $\tau_e$ . To encompass different cases of practical interest, we use three different deterministic functions

$$s_1(t) = -0.5 + t, \quad s_2(t) = \sin(2\pi t), \quad s_3(t) = \sin(6\pi t).$$

For each pair, the index  $r$  in (10) is drawn with equal probability from the set  $\{1, 2, 3\}$ . In order to make consistent estimation feasible, we represent each of the smooth functions in a cubic spline basis on 10 knots (equidistant on the unit interval).

Additionally, we draw the copula family for each pair-copula with equal probability from the Gaussian, Student  $t$  (with four degrees of freedom), Clayton and Gumbel families. The Clayton and Gumbel families are extended to allow for  $\tau < 0$  by using  $90^\circ$  and  $270^\circ$  rotations. For example, if  $c^{\text{Clay}}(u_1, u_2; \tau)$  denotes the Clayton copula density with  $\tau > 0$ , then  $c^{\text{Clay}90}(u_1, u_2; -\tau) = c(u_2, 1 - u_1; \tau)$  is its 90 degree (counter-clockwise) rotation and allows for negative dependence.

Finally, we repeat the experiment 1 000 times for each of the two sample sizes  $n = 500, 5\,000$ .

### 3.2 Results

In what follows, we discuss the results of the simulation study outlined above. In the two-dimensional case, the penalized likelihood estimator was found to perform well by Vatter & Chavez-Demoulin (2015): the pair-copulas from the first tree correspond to such a situation.

In other trees, estimates are based on pseudo-observations, so estimation errors from the first tree (and subsequent ones) are expected to propagate and damage the performance. Hence, emphasis is put on how this performance changes with the tree level. We split the analysis in three parts. The first two parts discuss respectively the accuracy of estimates for the linear coefficient and the smooth functions. The third part concerns the selection of copula families and covariates. We also investigated whether the copula family influences the estimation accuracy. Because the differences are tiny and do not lead to interesting insights, the results are not shown here.

#### Estimation of Linear Coefficients.

The accuracy of estimates of the linear coefficients  $\beta$  is illustrated in [Figure 3](#). The  $x$ -axis contains the ten entries of the vector  $\beta$ . For each  $\beta_j$  ( $j = 1, \dots, 10$ ), [Figure 3](#) shows four bars. Each bar represents the range from the 5% to the 95% quantiles of the 1000 estimated coefficients, and the mean is shown as a circle. The four bars correspond to the first to fourth tree level of the PCC (from left to right). Horizontal bars indicate the true value of the coefficient. The left column corresponds to the oracle estimator where copula family and covariates included in the model are correctly specified. The right column corresponds to estimates resulting from procedure described in [Section 2.4](#).

For the coefficients  $\beta_4, \beta_5, \beta_9, \beta_{10}$ , the estimation error of the oracle estimator is zero, because the correct model specification does not include  $z_4, z_5, z_9, z_{10}$ . In contrast, the estimates from the model selection procedure fluctuate around zero, with a variance decreasing with the sample size. Interestingly, the tree level does not appear to affect the variance.

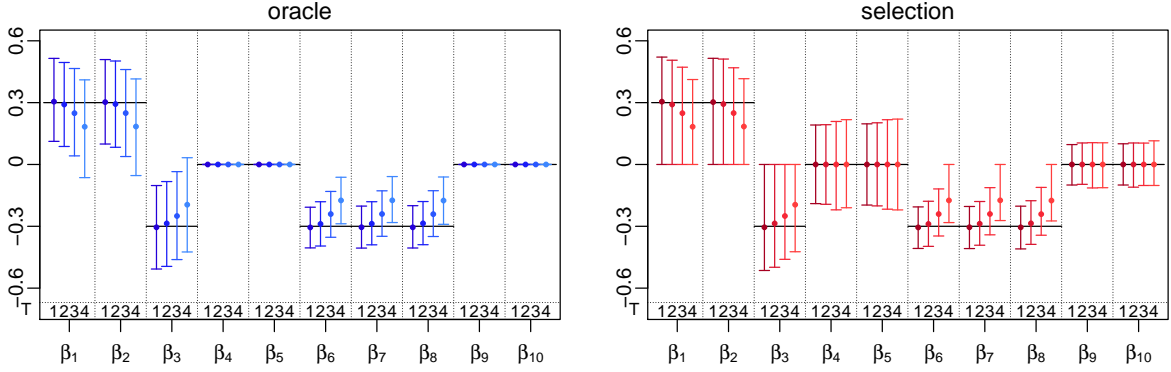
For the other coefficients, namely  $\beta_1, \beta_2, \beta_3, \beta_6, \beta_7, \beta_8$ , the variance is similarly decreasing with the sample size, but unaffected by the tree level. The estimators are also unbiased in the first tree, but this is not the case in subsequent trees. However, while the estimators are increasingly biased toward zero with the tree level, this effect decreases with the sample size, as expected. This shrinkage towards zero is a consequence of the sequential procedure: estimation errors in upper trees propagate and disguise the effects of covariates in subsequent trees. In other words, the bias increases because pseudo-observations in subsequent trees are obtained from estimates of the previous tree(s).

While this finite sample bias is puzzling, consistency of the sequential estimation can be easily established. Because the true model contains a finite number of parameters and each step is a likelihood maximization, the procedure can be viewed as  $\sqrt{n}$ -consistent and asymptotically normal generalized method of moments estimator (see [Newey & McFadden 1994](#), Chapter 6).

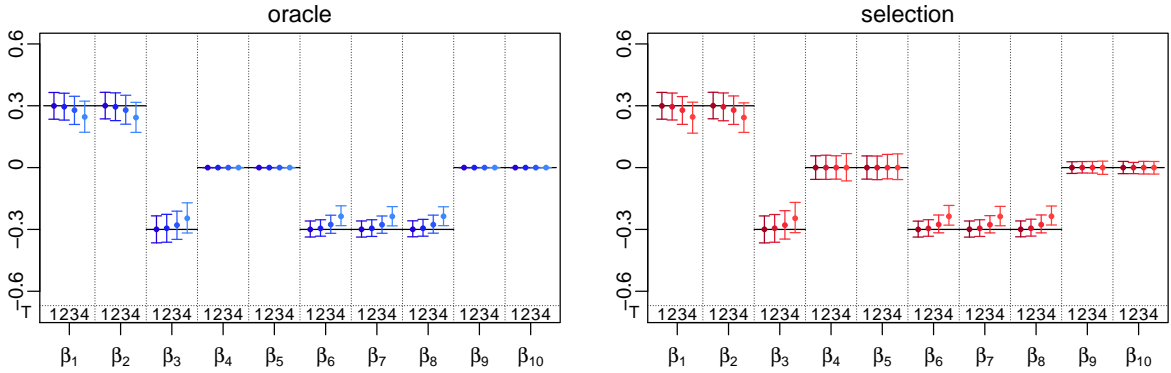
In parametric models with a large number of parameters, such shrinkage is often intentional to avoid overfitting (e.g., in the context of high-dimensional linear regression). In our case, the true model contains  $(4+3+2+1)$  (pair-copulas)  $\times$   $(10+6)$  (spline and linear coefficients) = 160 parameters. Even when a five-dimensional PCC contains a single linear covariate, there are  $10 \times 2$  parameters to estimate. So although the shrinkage that we observe is not intentional, it may be opportune.

#### Estimation of the Smooth Functions.

We now turn to the estimation of the smooth components  $s_r$  ( $r = 1, \dots, 3$ ), which are drawn as solid lines in each of the columns of [Figure 4a](#). The first,  $s_1$ , is a simple linear function;



(a)  $n = 500$

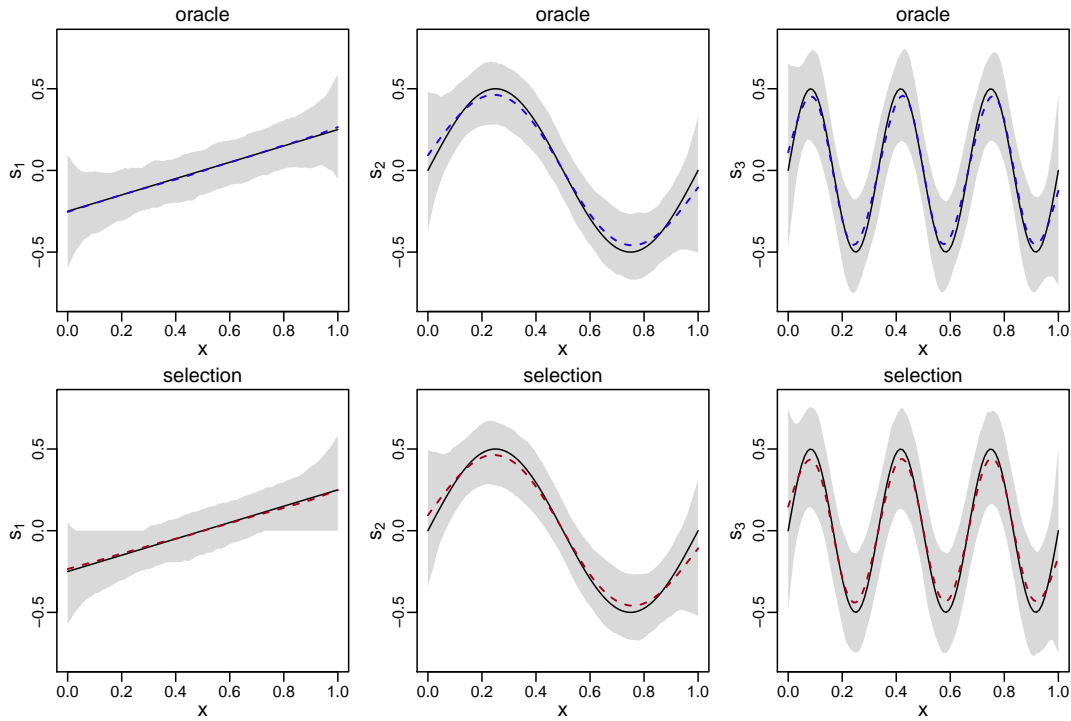


(b)  $n = 5000$

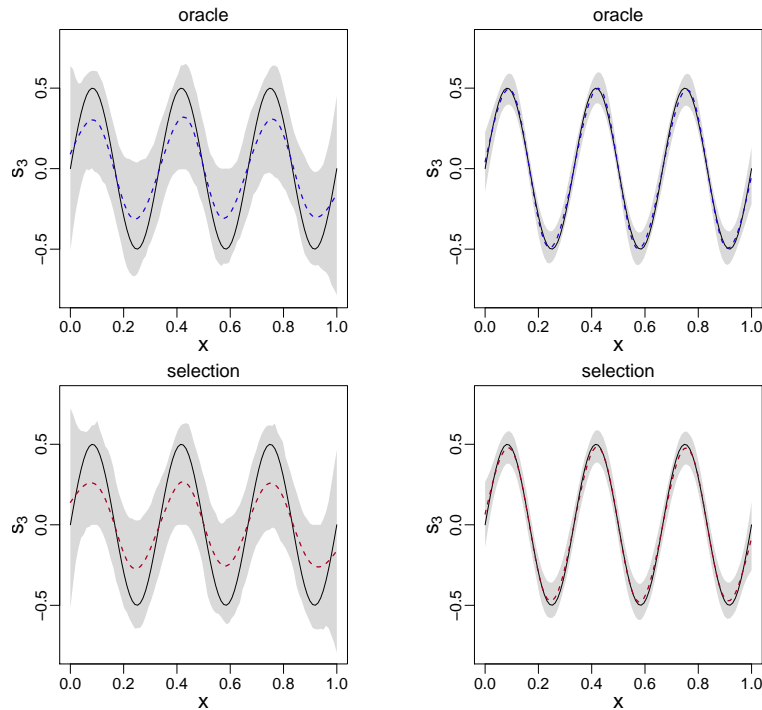
Figure 3: Estimation of the Linear Coefficients. The estimates using the correctly specified estimator (oracle) and the model selection algorithm (selection) are compared. For each coefficient  $\beta_j$  ( $j = 1, \dots, 10$ ), the results are split by tree level (i.e., 1, 2, 3 or 4). Mean estimates are indicated by circles. Bars represent the range from the 5% to the 95% quantiles.

$s_2$  and  $s_3$  are sines with one and three wave periods. They represent increasing complexity, and are expected to be increasingly difficult to estimate. Mean estimates for the first tree and  $n = 500$  are shown by dashed lines with pointwise ranges from the 5% to the 95% quantiles as shaded areas. The oracle and selection estimators are able to recover the three functions accurately. There is a small bias in regions where the functions display a high curvature. This is not surprising because a penalty is imposed on the second derivative of the fitted curves.

In Figure 4b, similarly as for the linear coefficients, a bias appears in the lower trees, which we only illustrate for  $s_3$  and the fourth tree to save space. For  $n = 500$  (left column), both the oracle and selection estimators are biased towards zero. Furthermore, the bias is larger for the latter, because the number of knots is also selected automatically. Often, fewer than ten knots are selected, and since the true function cannot be represented by such a basis, this causes additional bias. However, the bias almost completely vanishes for  $n = 5000$  (right column) for both the oracle and selection estimators.



(a) Estimation of  $s_1, s_2, s_3$  in Tree  $T_1$  with  $n = 500$ .



(b) Estimation of  $s_3$  in Tree  $T_4$  with  $n = 500$  (left column) and  $n = 5000$  (right column).

Figure 4: Estimation of the Smooth Functions. The estimates using the correctly specified estimator (oracle) and the model selection algorithm (selection) are compared. The true calibration function is the solid line, along with the mean estimates (dashed lines) and pointwise range from the 5% to the 95% quantiles (shaded area).

Model Selection.

Table 1 shows the frequency that the true family is selected, split by sample size and tree. Selecting the true family in about 90% of the cases in the first and 50% of the cases in the fourth tree, the method seems to work, though the performance deteriorates in lower trees.

Table 1: Frequencies of the true copula family being selected (in %). Results are split by sample size and tree level. Standard errors are given in brackets below.

$n$	$T_1$	$T_2$	$T_3$	$T_4$
500	92.2 (0.4)	86.0 (0.6)	70.8 (1.0)	56.3 (1.6)
5 000	94.4 (0.4)	94.4 (0.4)	82.5 (0.8)	55.8 (1.6)

For  $n = 500$ , Table 2 and Table 3 are contingency tables with the frequency for each family to be chosen correctly. In the first tree (Table 2), the family selection works well for the Student  $t$ , Clayton, and Gumbel families. When the true copula family is Gaussian, the Student  $t$  copula is selected in  $2.5/23.9 \approx 10\%$  of the cases. In the fourth tree (Table 3), the performance deteriorates, and the Student  $t$  copula is more than 30% of the time when the true copula is Gaussian. In fact, even when the true copula is Archimedean, elliptical copulas are selected roughly 60% of the time. Although not shown here, both effects decrease with the sample size.

Table 2: Contingency table with frequencies for each family to be selected for  $n = 500$  and tree  $T_1$  (in %).

selected family	true family				$\Sigma$
	Gaussian	Student $t$	Clayton	Gumbel	
Gaussian	20.9	0.2	0.4	1.5	22.9
Student $t$	2.5	23.8	0.4	1.7	28.4
Clayton	0.0	0.0	25.3	0.0	25.3
Gumbel	0.6	0.5	0.0	22.3	23.4
$\Sigma$	23.9	24.5	26.1	25.5	100.0

Recall that the family is chosen based on the AIC, a trade-off between goodness of fit and model complexity. In a finite sample, the likelihood of the Student  $t$  copula is necessarily larger than that of the Gaussian copula, because the former nests the latter. On the other hand, the AIC puts a larger penalty on the Student  $t$  copula for the additional parameter. However, the GAM for a single pair-copula usually has more than ten parameters to account for the covariate effects. Hence, the increase in penalty resulting from selecting Student  $t$  copula over the Gaussian is relatively small. This is only a minor problem, since the two families are very similar overall. As for the selection of the Student  $t$  copula when the true family is Archimedean, the true model for each pair-copula is specified for the Kendall's  $\tau$ . Hence, while some distributional features such as Archimedean's tail asymmetries cannot be reproduced by the Student  $t$  copula, the covariate effects on Kendall's  $\tau$  can.

Table 3: Contingency table with frequencies for each family to be selected for  $n = 500$  and tree  $T_4$  (in %).

selected family	true family				$\Sigma$
	Gaussian	Student $t$	Clayton	Gumbel	
Gaussian	11.3	0.9	5.2	4.7	22.1
Student $t$	7.8	23.1	10.0	6.9	47.8
Clayton	0.8	0.6	10.6	0.2	12.2
Gumbel	4.0	1.9	0.7	11.3	17.9
$\Sigma$	23.9	26.5	26.5	23.1	100.0

Finally, we investigate the automatic selection of the covariates. Table 4 shows the frequency that a covariate was correctly included or excluded from the model (averaged over all eleven covariates). For the choice of covariates, a correct selection means that  $Z_1, Z_2, Z_3, Z_6, Z_7, Z_8,$  and  $t$  are included, and that  $Z_4, Z_5, Z_9,$  and  $Z_{10}$  are not. Again, we observe that the performance decreases with the tree level (e.g., from 90% in the first tree to 50% in the fourth for  $n = 500$ ), and increases with the sample size (e.g., from 50% for  $n = 500$  to 90% for  $n = 5000$  in the fourth tree). We conclude that the model selection algorithm works reasonably well, although there may be room for improvement, especially regarding family selection.

Table 4: Frequencies of the correct choice of covariates (in %). Results are split by sample size and tree level. Standard errors are given in brackets below.

$n$	$T_1$	$T_2$	$T_3$	$T_4$
500	89.1 (0.2)	88.1 (0.2)	82.3 (0.3)	71.9 (0.4)
5 000	94.0 (0.1)	93.7 (0.1)	93.2 (0.2)	90.8 (0.3)

## 4 APPLICATION

We use the methodology developed in this paper to study the cross-sectional dynamics of intraday asset returns. They offer a magnifying glass to study financial markets while posing unprecedented econometric challenges. More specifically, we focus on the foreign exchange (FX) market, which determines the relative value of currencies. The two main characteristics of this decentralized market are that it operates both around the clock (from Sunday 10pm to Friday 10pm UTC) and around the globe (i.e., it is geographically dispersed). Recently, [Vatter & Chavez-Demoulin \(2015\)](#) observed that the intraday dependence structure pattern, due to the cyclical nature of market activity, is shaped similarly to that of the univariate conditional second moments.

In what follows, we extend their bivariate model to encompass three or more exchange rates using vines with exogenous covariates. We use data graciously provided by Dukascopy

Bank SA ([www.dukascopy.com](http://www.dukascopy.com)), an electronic broker holding a Securities Dealer License issued by the FINMA. It contains 15-minute spaced returns (i.e., 96 observations each day) for the EURUSD, GBPUSD, USDCHF, and USDJPY, from March 10, 2013 to November 1, 2013. Hence, in a total of 34 trading weeks, there are 16320 observations (170 days) excluding weekends.

## 4.1 Modeling the Marginal Distributions

Because intraday returns are heteroskedastic, we need to pre-filter the individual series before applying the methodology of this paper. In this context, the high-frequency econometrics literature usually decomposes the volatility in two multiplicative components: a seasonal, but often assumed deterministic, and a stochastic part (see e.g., [Andersen & Bollerslev 1997, 1998](#), [Engle & Sokalska 2012](#)). It is straightforward to achieve this within the GARCH-family, where  $r_t = \sigma_t y_t$  for  $\sigma_t$  a function of  $\{r_{t-1}, \sigma_{t-1}, r_{t-2}, \sigma_{t-2}, \dots\}$  and  $y_t$  a white noise, which we do by writing

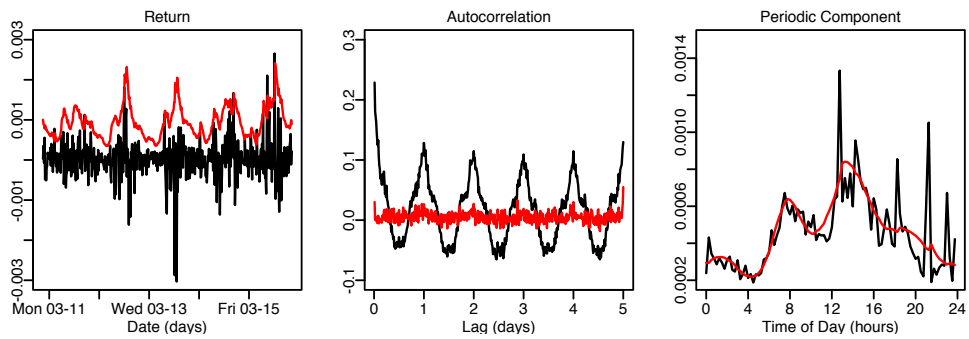
$$\log \sigma_t^2 = \left[ \omega + \sum_{k=1}^K \{a_k \cos(2\pi kt/T) + b_k \sin(2\pi kt/T)\} \right] + \alpha \epsilon_{t-1} + \gamma (|\epsilon_{t-1}| - \mathbb{E}|\epsilon_{t-1}|) + \beta \log \sigma_{t-1}^2,$$

where  $T = 96$ . This model is the EGARCH(1,1) from [Nelson \(1991\)](#), augmented with external regressors to take the seasonality into account. The sum of cosines and sines with integer frequencies, designed to capture daily oscillations around the base level, is similar to the Fourier Flexible Form (FFF, see [Gallant 1981](#)), introduced in this context by [Andersen & Bollerslev \(1997, 1998\)](#). Denoting by  $\hat{\sigma}_t$  the fitted volatility using the maximum log-likelihood estimator with  $K = 5$ , we call  $\hat{y}_t = r_t / \hat{\sigma}_t$  the residuals.

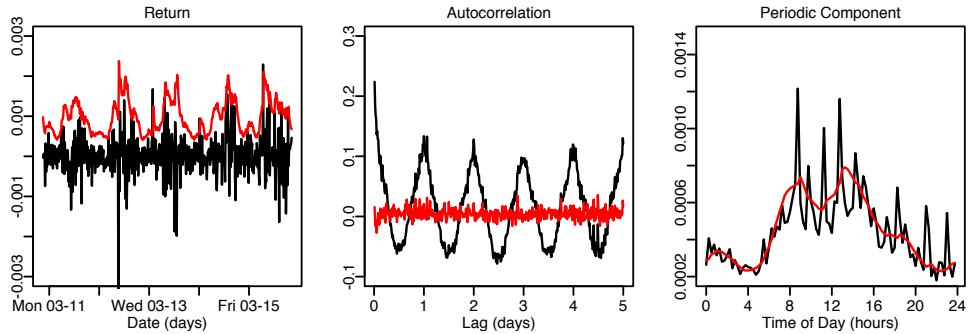
In the left panels of [Figure 5](#), we show the returns,  $r_t$ , along with two fitted conditional standard deviations,  $2 \times \hat{\sigma}_t$ , for each exchange rate for the first week. In the middle panels of [Figure 5](#), the black (respectively red) curve represents the autocorrelation of the absolute value of the returns (respectively residuals), where we observe that our univariate models appropriately capture the heteroskedasticity. In the right panels of [Figure 5](#), the black (respectively red) curve represents the empirical (respectively fitted) volatility per 15-minute bin, where we recognize the usual modes at the opening time of the Tokyo, London and New-York markets.

## 4.2 Modeling the Dependence Structure

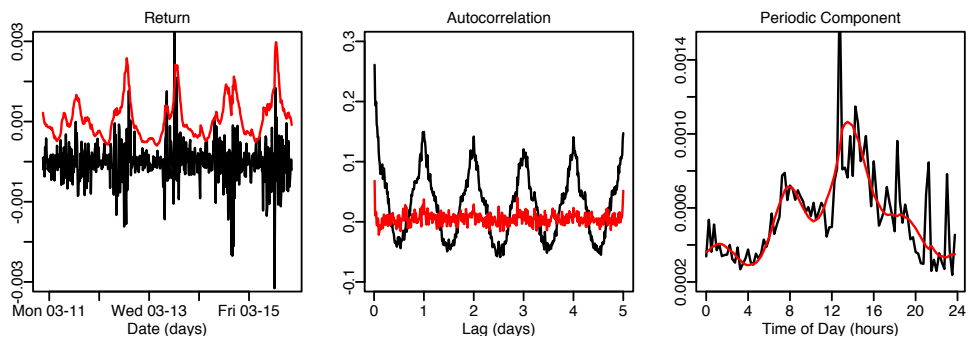
From the residuals, we compute observations on the copula scale by using the empirical cumulative distribution for each individual time series. We use the same FFF regressors to model the periodic component of the dependence structure. We also add a smooth function of time  $t$ , to model the evolution of the dependence over the sample period. We then run the procedure described in [Section 2.4](#). The resulting fitted model for the corresponding



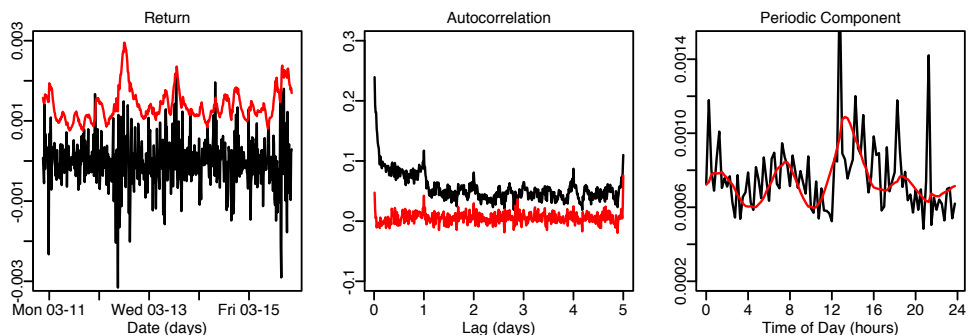
(a) EURUSD



(b) GBPUSD



(c) USDCHF



(d) USDJPY

Figure 5: Marginal modeling of the Four FX rates. In the left panels, the return,  $r_t$ , (black line) and two conditional standard deviations,  $2 \times \hat{\sigma}_t$ , (red line) are shown for the first week of the sample. In the middle panels, the autocorrelation of the absolute value of the return/deseasonalized residual are the black/red lines. In the right panels, the black (respectively red) curve represents the empirical (respectively fitted) volatility per 15-minute bin.

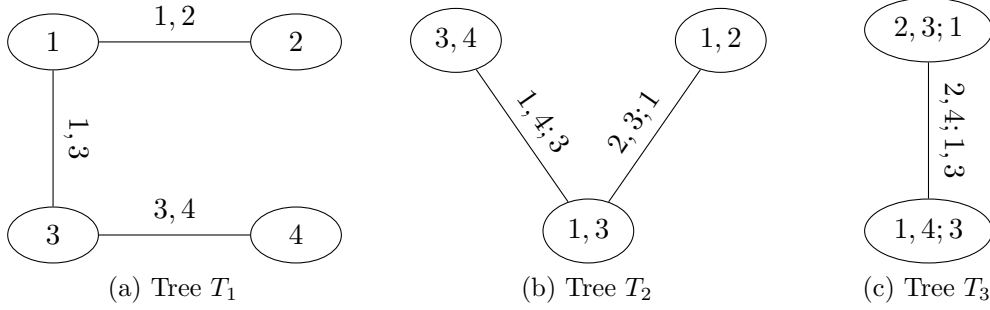


Figure 6: The Regular Vine Tree Sequence for the Four FX rates. The numbers represent the FX rates (EURUSD: 1; GBPUSD: 2; USDCHF: 3; USDJPY: 4),  $x, y$  denote the bivariate distribution of  $x$  and  $y$ , and  $x, y, z$  denote the bivariate distribution of  $x$  and  $y$  conditional on  $z$ . Each edge corresponds to a bivariate pair-copula in the PCC.

conditional pair-copulas can be written as

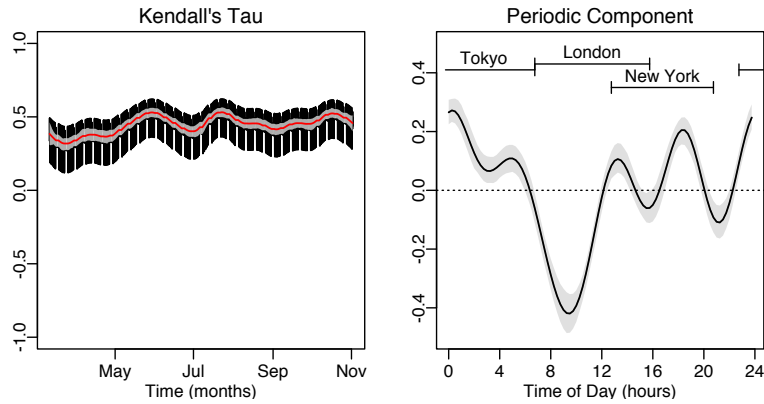
$$\begin{aligned}
 \tau_{1,2}(\mathbf{w}) &= g_{1,2} \left\{ \mathbf{x}(t)^\top \boldsymbol{\beta}_{1,2} + s_{1,2}(21.13, t) \right\}, \\
 \tau_{1,3}(\mathbf{w}) &= g_{1,3} \left\{ \mathbf{x}(t)^\top \boldsymbol{\beta}_{1,3} + s_{1,3}(63.12, t) \right\}, \\
 \tau_{3,4}(\mathbf{w}) &= g_{3,4} \left\{ \mathbf{x}(t)^\top \boldsymbol{\beta}_{3,4} + s_{3,4}(58.25, t) \right\}, \\
 \tau_{2,3;1}(\mathbf{w}) &= g_{2,3;1} \left\{ \mathbf{x}(t)^\top \boldsymbol{\beta}_{2,3;1} + s_{2,3;1}(9.53, t) \right\}, \\
 \tau_{1,4;3}(\mathbf{w}) &= g_{1,4;3} \left\{ \mathbf{x}(t)^\top \boldsymbol{\beta}_{1,4;3} + s_{1,4;3}(27.96, t) \right\}, \\
 \tau_{2,4;1,3}(\mathbf{w}) &= g_{2,4;1,3} \left\{ \mathbf{x}(t)^\top \boldsymbol{\beta}_{2,4;1,3} + s_{2,4;1,3}(21.77, t) \right\},
 \end{aligned}$$

where  $\mathbf{x}(t) = (1, \cos(2\pi t/T), \dots, \cos(2\pi 5t/T), \sin(2\pi t/T), \dots, \sin(2\pi 5t/T))^\top$ , 1 = EURUSD, 2 = GBPUSD, and 3 = USDCHF, and 4 = USDJPY, and the first number in each smooth function corresponds to the estimated EDF. As is often the case with financial data, the Student  $t$  copula is selected by both the AIC and BIC for all conditional pair-copulas over the Gaussian or common Archimedean copulas.

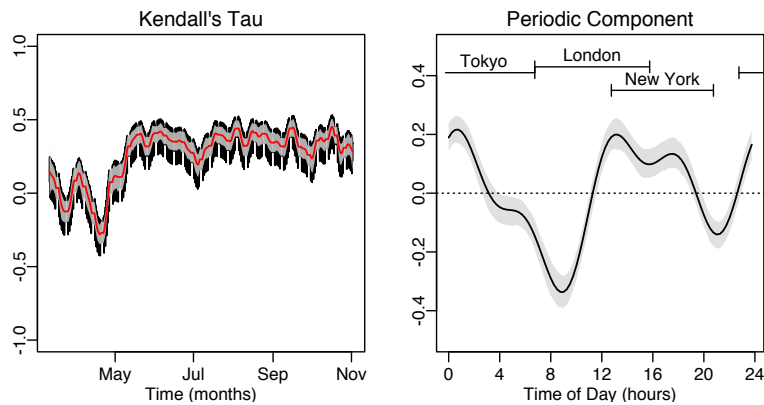
In Figures 7 and 8, we show all fitted smooth and periodic components (without the intercept). In the left panels of both figures, the sum of the smooth and the periodic components, that is  $g \left\{ \mathbf{x}(t)^\top \hat{\boldsymbol{\beta}} + \hat{s}(t) \right\}$  is the black line, oscillating wildly because of the daily periodicity. For the sake of clarity, we also show  $g \left\{ \hat{s}(t) \right\}$  with bootstrapped 95% confidence bands as the red line with shaded grey area. In this case, we assume that  $\mathbf{x}(t)^\top \hat{\boldsymbol{\beta}} = 0$ , which is sensible since the periodic component averages zero over one day. Finally, in the right panels, we show the periodic component only (black line), on the scale of the linear predictor, that is  $\mathbf{x}(t)^\top \hat{\boldsymbol{\beta}}$ , with bootstrapped 95% confidence bands (shaded grey area).

#### Dependence Analysis for the First Tree.

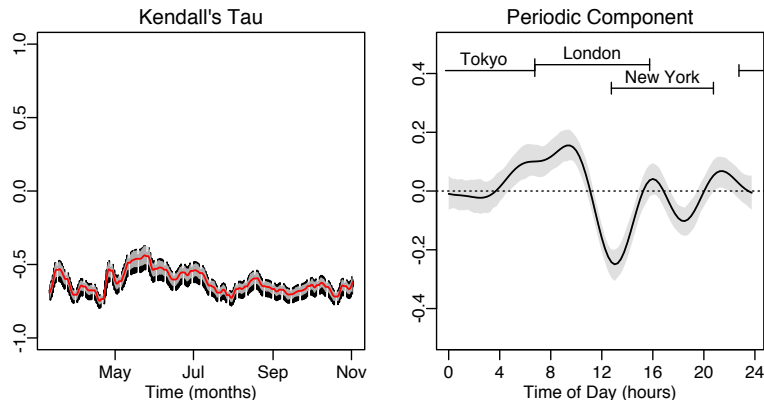
In the first tree (i.e., the first three pair-copulas), a pair-copula describes directly the time-varying dependence between two currency pairs. For instance, the red curve in each of the left panels of Figures 7a, 7b and 7c illustrates the long-term evolution of Kendall's  $\tau$ .



(a) Smooth and Periodic Component for the GBPUSD-EURUSD copula.

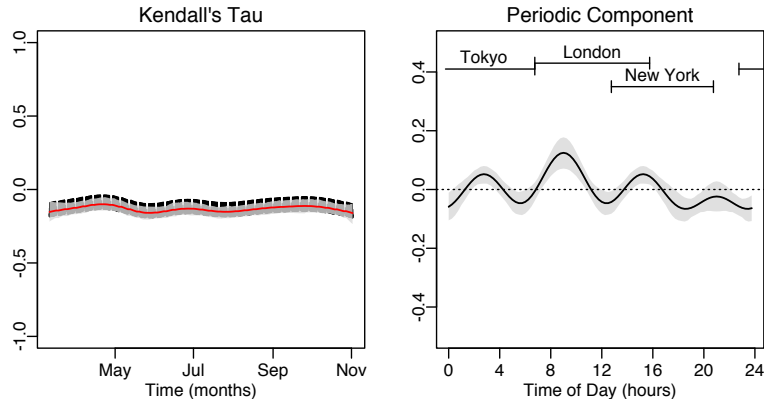


(b) Smooth and Periodic Component for the USDJPY-USDCHF copula.

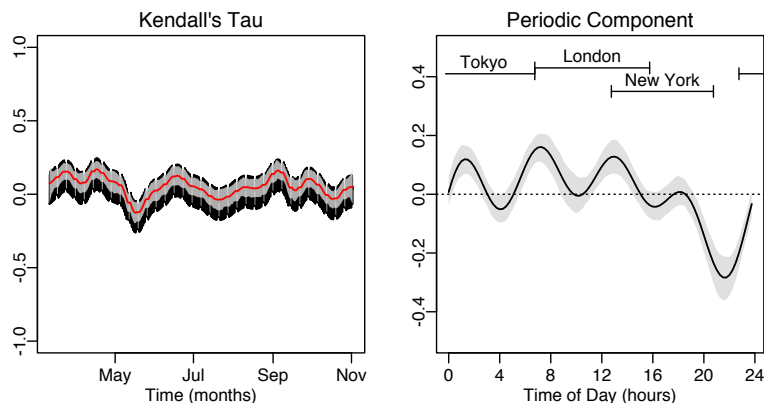


(c) Smooth and Periodic Component for the EURUSD-USDCHF copula.

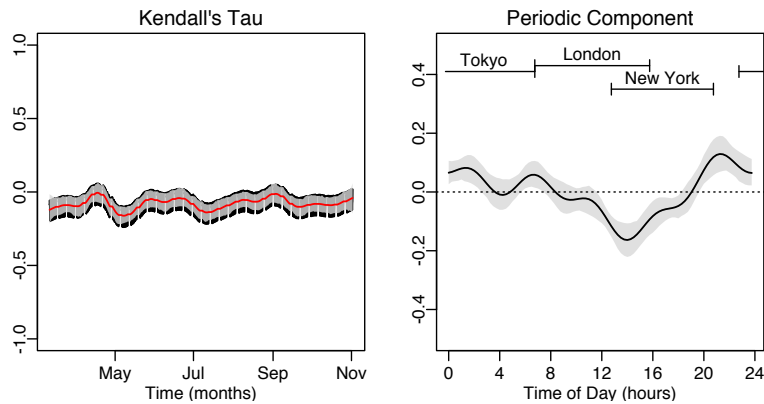
Figure 7: Results for the First Tree of the PCC for the Four FX rates. In the left panels, the sum of the smooth and the periodic components is the black line, and the smooth component with its 95% confidence band is the red line with shaded grey area. All quantities are shown on the Kendall's  $\tau$  scale. In the right panels, the periodic component with its 95% confidence band is the black line with shaded grey area. All quantities are shown on the linear predictor scale.



(a) Smooth and Periodic Component for the GBPUSD-USDCHF;EURUSD copula.



(b) Smooth and Periodic Component for the EURUSD-USDJPY;USDCHF copula.



(c) Smooth and Periodic Component for the GBPUSD-USDJPY;USDCHF;EURUSD copulas.

Figure 8: Results for the Second and Third Trees of the PCC for the Four FX rates. In the left panels, the sum of the smooth and the periodic components is the black line, and the smooth component with its 95% confidence band is the red line with shaded grey area. All quantities are shown on the Kendall's  $\tau$  scale. In the right panels, the periodic component with its 95% confidence band is the black line with shaded grey area. All quantities are shown on the linear predictor scale.

We observe that the dependence is positive for GBPUSD-EURUSD and USDJPY-USDCHF, but negative for EURUSD-USDCHF. Similarly, the patterns in the right panels of [Figure 7c](#) essentially mirror the one of [Figures 7a](#) and [7b](#). The explanation lies in the position of the USD in the currency pairs. In the GBPUSD-EURUSD, the USD is the second leg of both rates, while in the USDJPY-USDCHF, the USD is the first leg of both rates. Conversely, for the EURUSD-USDCHF, the USD appears as the first and second leg of each exchange rate. The absolute valuation of the USD is mainly related to the health of the US economy. Hence, when a piece of information which the market interprets as positive for the US economy is released (e.g., a diminishing unemployment rate), the USD becomes more valuable. When this is the case, the GBPUSD and EURUSD both decrease, and the USDJPY and USDCHF both increase. Since, in the GBPUSD-EURUSD and USDJPY-USDCHF, the USD is priced by the two legs in the same direction, the dependence is positive. Conversely, in the EURUSD-USDCHF, the USD is priced by the two legs in opposite directions, and the dependence is negative.

For the right panels of [Figures 7a](#), [7b](#) and [7c](#), we see two local peaks at the opening and closing of the US market. For the GBPUSD-EURUSD and USDJPY-USDCHF, respectively the EURUSD-USDCHF, the peaks are positive, respectively negative, that is of the same sign as the overall dependence. In other word, the absolute dependence is increased at the opening and closing of the US market, which represents evidence that the USD's valuation is a driver of the dependence between exchange rates. Comparatively, the absolute dependence becomes smaller when the London market opens or closes. This is interesting, because it contradicts the pattern observed in the volatility, where peaks were observed at the openings of the Asian, European, and US markets.

#### Dependence Analysis for the Subsequent Trees.

In the second and third trees, a pair-copula describes the dependence between two currency pairs after the effect of other currency pairs has been removed. For example, the pair copula for EURUSD-USDJPY;USDCHF is the residual dependence between EURUSD and USDJPY, once the dependence induced by the USDCHF has been removed. The USD always appears in one leg of the currency pairs whose influence is removed. Hence, we expect the USD to be less influential in the second and third trees.

Firstly, we observe that the long-term evolution become less relevant. Not only the red curves in the left panels of [Figures 8a](#), [8b](#) and [8c](#) are much smoother than in those of [Figures 7a](#), [7b](#) and [7c](#), they are also much closer to zero. Comparing [Figures 8a](#) and [8b](#), the conditional pair involving the GBPUSD is less wiggly than the one involving the USDJPY. The explanation comes from [Figures 7a](#) and [7b](#), where the same effect is observed: the pair involving the USDJPY (i.e., the USDJPY-USDCHF) is more wiggly than the one involving the GBPUSD (i.e., the GBPUSD-EURUSD).

Secondly, we still see significant periodic patterns in all pairs. For instance, in the right panel of [Figure 8a](#) (i.e., the EURUSD-USDJPY;USDCHF pair-copula), we observe positive dependence peaks at opening and closing times of the Tokyo and London markets. So after the influence of the USDCHF pair has been removed, the EURUSD and USDJPY appear to be positively dependent when the European and Japanese markets dominate the trading. Conversely, when both the London and Tokyo markets are closed, the dependence becomes more negative, which is likely caused by the opposite positioning of the USD in each pair.

In [Figure 8b](#) (i.e., the GBPUSD-USDCHF;EURUSD pair-copula), we see two small peaks at the opening and closing of the London market, suggesting that information about the European economies induces positive dependence between GBPUSD and USDCHF. Lastly, the right panel of [Figure 8c](#) (i.e., the GBPUSD-USDJPY;USDCHF,EURUSD pair-copula) exhibits positive dependence whenever neither London nor New York is trading, and negative dependence during New York’s opening hours. However, such a complex (second-order and non-linear) dependence relationship is rather difficult to interpret.

Summary.

In summary, we found strong evidence for a dynamic dependence structure in intraday foreign exchange rates. Our analysis suggests that it is appropriate to decompose the time-varying dependence into two components. The first captures the long-term evolution of the dependence. The second captures the daily patterns stemming from the periodic nature of the market, which is related to the opening and closing times of various exchanges around the world. This analysis is similar to the well-known patterns in the intraday volatility observed in the individual returns on intraday foreign exchange rates.

## 5 DISCUSSION

In this paper, we extend pair-copula constructions (PCCs) by letting the Kendall’s tau of each pair-copula be a function of covariates. We utilize the flexibility of generalized additive models (GAMs), which allow for parametric, semi-parametric or non-parametric specifications of the relationship between strength of dependence and the covariates. Building on the maximum penalized log-likelihood estimator for conditional copulas of [Vatter & Chavez-Demoulin \(2015\)](#), we propose a sequential estimation algorithm, as well as a heuristic method for a fully automatic model selection. We evaluate both in a simulation study, and we find that

- the estimates are unbiased in the first tree, but there is a shrinkage towards zero of increasing size in subsequent trees,
- the performance of the selection and estimation are comparable to that of an oracle estimator (where the structure and copula families are known),
- the model selection heuristic selects the true copula family and covariates most of the time, but the frequency gets smaller with increasing tree level.

We used this methodology to model the dependence between intraday returns of four exchange rates. We observed that the bivariate results of [Vatter & Chavez-Demoulin \(2015\)](#) extend directly in this higher-dimensional example. In other words, the data suggest that the dependence can be decomposed into a smooth and a periodic component. Furthermore, the periodic component for each conditional pair-copula has peaks that correspond to openings and/or closings of markets around the world. While most of the time-varying features are captured in the first tree, there is still a significant amount of periodicity left in the second and third trees of the PCC model.

The simulations and application presented in this paper feature only a medium number of covariates. When the number of covariates grows very large, the algorithms used in our approach may be very slow and run into numerical difficulties. To alleviate this, we could use a dimension reduction technique to reduce the dimensionality of the covariates. However, a reasonable method would have to be specifically tailored to the problem of conditional dependence modeling. To the best of our knowledge, no such method has been proposed yet. Although out of the scope of this paper, this promising approach is currently under investigation.

## **ACKNOWLEDGEMENTS**

The authors would like to thank for useful comments and discussions Valérie Chavez-Demoulin, Claudia Czado, and Anthony Davison, as well as participants from the 2016 conference on Dependence Modeling in Finance, Insurance and Environmental Science in Munich.

# APPENDIX: MODEL SELECTION ALGORITHM FOR A SINGLE COPULA FAMILY

In [Algorithm 1](#), we use *PMLE*, a function which computes the penalized maximum log-likelihood estimator  $\hat{\theta}$  while selecting the vector of smoothing parameters  $\gamma$  automatically using GVC minimization (cf., [Vatter & Chavez-Demoulin 2015](#)). Its inputs are two  $n \times 1$  vectors (say  $u_1$  and  $u_2$ ), a  $n \times k$  matrix of  $k$  covariates, and a  $k \times 1$  vector of basis sizes for the smooth components corresponding to each covariates. Its output is the fitted model.

---

**Algorithm 1** Model selection for a bivariate conditional copula with known family

---

```

1: Inputs:
    $u_1, u_2, y_1, \dots, y_k, \alpha$ 
2: Initialize:
    $b \leftarrow k$ 
    $basis_j \leftarrow 10, j = 1, \dots, b$ 
    $cov \leftarrow$  a  $n \times b$  matrix with columns  $y_1, \dots, y_b$ 
    $sel \leftarrow false$ 
3: while ANY( $sel \neq true$ ) AND  $b > 0$  do ▷ Remove the “insignificant” covariates
4:    $fitted \leftarrow PMLE(u_1, u_2, cov, basis)$ 
5:   Clear  $basis$ ,  $PV$ , and  $sel$ 
6:    $PV_j \leftarrow$   $p$ -value of  $fitted$  corresponding to column  $j$  of  $cov, j = 1, \dots, b$ 
7:    $sel_j \leftarrow true, j = 1, \dots, b$ 
8:   for  $j = 1$  to  $b$  do
9:     if  $PV_j \geq \alpha$  then
10:       $sel_j \leftarrow false$ 
11:      remove column  $j$  from  $cov$ 
12:    end if
13:  end for
14:   $b \leftarrow \sum_{j=1}^b \mathbb{1}_{PV_j < \alpha}$ 
15:   $basis_j \leftarrow 10, j = 1, \dots, b$ 
16: end while
17:  $fitted \leftarrow PMLE(u_1, u_2, cov, basis)$ 
18: if  $b \neq 0$  then ▷ Select the basis size
19:    $EDF_j \leftarrow$  EDF of  $fitted$  corresponding to column  $j$  of  $cov, j = 1, \dots, b$ 
20:   if ANY( $EDF > basis \times 0.8$ ) then
21:     while ANY( $sel == true$ ) AND ALL( $basis < n/30$ ) do
22:       Clear  $sel$ 
23:        $sel_j \leftarrow false, j = 1, \dots, b$ 
24:       for  $j = 1$  to  $b$  do
25:         if  $EDF_j > basis \times 0.8$  then
26:            $sel_j \leftarrow true$ 
27:            $basis_j \leftarrow 2 \cdot basis_j$ 
28:         end if
29:       end for
30:        $fitted \leftarrow PMLE(u_1, u_2, cov, basis)$ 
31:        $EDF_j \leftarrow$  EDF of  $fitted$  corresponding to column  $j$  of  $cov, j = 1, \dots, b$ 
32:     end while
33:   end if
34: end if
35: return  $fitted$ 

```

---

## SUPPLEMENTARY MATERIAL

**R-package “gamCopula”:** The package contains inference and simulation tools to apply GAMs to bivariate copulas and PCCs. (GNU zipped tar file)

## REFERENCES

- Aas, K., Czado, C., Frigessi, A. & Bakken, H. (2009), “Pair-Copula Constructions of Multiple Dependence”, *Insurance: Mathematics and Economics* **44**(2), 182–198.
- Acar, E., Craiu, R. & Yao, F. (2011), “Dependence Calibration in Conditional Copulas: a Nonparametric Approach”, *Biometrics* **67**, 445–453.
- Acar, E. F., Genest, C. & Nešlehová, J. (2012), “Beyond Simplified Pair-Copula Constructions”, *Journal of Multivariate Analysis* **110**, 74–90.
- Andersen, T. G. & Bollerslev, T. (1997), “Intraday Periodicity and Volatility Persistence in Financial Markets”, *Journal of Empirical Finance* **4**(2-3), 115–158.
- Andersen, T. G. & Bollerslev, T. (1998), “Deutsche Mark – Dollar Volatility : Intraday Activity Patterns, Macroeconomic Announcements, and Longer Run Dependencies”, *The Journal of Finance* **53**(1), 219–265.
- Bedford, T. & Cooke, R. M. (2001), “Probability Density Decomposition for Conditionally Dependent Random Variables Modeled by Vines”, *Annals of Mathematics and Artificial Intelligence* **32**(1-4), 245–268.
- Bedford, T. & Cooke, R. M. (2002), “Vines – A New Graphical Model for Dependent Random Variables”, *The Annals of Statistics* **30**(4), 1031–1068.
- Craiu, R. V. & Sabeti, A. (2012), “In Mixed Company: Bayesian Inference for Bivariate Conditional Copula Models with Discrete and Continuous Outcomes”, *Journal of Multivariate Analysis* **110**, 106–120.
- Craven, P. & Wahba, G. (1979), “Smoothing Noisy Data with Spline Functions: Estimating the Correct Degree of Smoothing by the Method of Generalized Cross-validation”, *Numerische Mathematik* **31**(4), 377–403.
- Czado, C. (2010), Pair-Copula Constructions of Multivariate Copulas, in P. Jaworski, F. Durante, W. K. Härdle & T. Rychlik, eds, “Copula Theory and Its Applications”, Lecture Notes in Statistics, Springer Berlin Heidelberg, pp. 93–109.
- Engle, R. F. & Sokalska, M. E. (2012), “Forecasting Intraday Volatility in the US Equity Market. Multiplicative Component GARCH”, *Journal of Financial Econometrics* **10**(1), 54–83.
- Erhardt, T. M., Czado, C. & Schepsmeier, U. (2015a), “R-vine Models for Spatial Time Series with an Application to Daily Mean Temperature”, *Biometrics* **71**(2), 323–332.

- Erhardt, T. M., Czado, C. & Schepsmeier, U. (2015*b*), “Spatial Composite Likelihood Inference Using Local C-vines”, *Journal of Multivariate Analysis* **138**, 74–88.
- Gallant, R. (1981), “On the Bias in Flexible Functional Forms and an Essentially Unbiased Form: The Fourier Flexible Form”, *Journal of Econometrics* **15**(2), 211–245.
- Gijbels, I., Veraverbeke, N. & Omelka, M. (2011), “Conditional Copulas, Association Measures and Their Applications”, *Computational Statistics and Data Analysis* **55**, 1919–1932.
- Gräler, B. (2014), “Modelling Skewed Spatial Random Fields Through the Spatial Vine Copula”, *Spatial Statistics* **10**, 87–102.
- Green, P. J. & Silverman, B. W. (2000), *Nonparametric Regression and Generalized Linear Models – a Roughness Penalty Approach*, Chapman & Hall/CRC.
- Haff, I., Aas, K. & Frigessi, A. (2010), “On the Simplified Pair-copula Construction - Simply Useful or Too Simplistic?”, *Journal of Multivariate Analysis* **101**(5), 1296–1310.
- Härdle, W. & Liang, H. (2007), *Partially Linear Models*, Springer-Verlag New York.
- Hastie, T. J. & Tibshirani, R. J. (1990), *Generalized Additive Models*, Chapman & Hall/CRC.
- Hobæk Haff, I. (2013), “Parameter Estimation for Pair-copula Constructions”, *Bernoulli* **19**(2), 462–491.
- Joe, H. (1997), *Multivariate Models and Dependence Concepts*, Chapman & Hall/CRC.
- Marra, G. & Wood, S. N. (2012), “Coverage Properties of Confidence Intervals for Generalized Additive Model Components”, *Scandinavian Journal of Statistics* **39**(1), 53–74.
- Nagler, T. & Czado, C. (2016), “Evading the Curse of Dimensionality in Nonparametric Density Estimation with Simplified Vine Copulas”, *arXiv:1503.03305v3 [stat.ME]* .
- Nelsen, R. B. (2006), *An Introduction to Copulas*, Springer-Verlag New York.
- Nelson, D. B. (1991), “Conditional Heteroskedasticity in Asset Returns: A New Approach”, *Econometrica* **59**(2), 347–370.
- Newey, W. K. & McFadden, D. (1994), Large Sample Estimation and Hypothesis Testing, in R. F. Engle & D. L. McFadden, eds, “Handbook of Econometrics”, Elsevier North Holland, pp. 2111–2245.
- Nychka, D. (1988), “Bayesian Confidence Intervals for Smoothing Splines”, *Journal of the American Statistical Association* **83**(404), 1134–1143.
- Patton, A. J. (2002), Applications of Copula Theory in Financial Econometrics, PhD thesis, University of California, San Diego.

- Requena, A. I., Mediero, L. & Garrote, L. (2013), “A Bivariate Return Period Based on Copulas for Hydrologic Dam Design: Accounting for Reservoir Routing in Risk Estimation”, *Hydrology and Earth System Sciences* **17**(8), 3023–3038.
- Sabeti, A., Wei, M. & Craiu, R. V. (2014), “Additive Models for Conditional Copulas”, *Stat* **3**(1), 300–312.
- Sklar, A. (1959), “Fonctions de Répartition à n Dimensions et Leurs Marges”, *Publications de L’Institut de Statistique de L’Université de Paris* **8**, 229–231.
- Spanhel, F. & Kurz, M. S. (2015), “Simplified Vine Copula Models: Approximations Based on the Simplifying Assumption”, *arXiv:1510.06971 [stat.ME]*.
- Stöber, J. & Czado, C. (2014), “Regime Switches in the Dependence Structure of Multidimensional Financial Data”, *Computational Statistics & Data Analysis* **76**, 672–686.
- Stöber, J., Joe, H. & Czado, C. (2013), “Simplified Pair Copula Constructions — Limitations and Extensions”, *Journal of Multivariate Analysis* **119**, 101–118.
- Vatter, T. & Chavez-Demoulin, V. (2015), “Generalized Additive Models for Conditional Dependence Structures”, *Journal of Multivariate Analysis* **141**, 147–167.
- Veraverbeke, N., Omelka, M. & Gijbels, I. (2011), “Estimation of a Conditional Copula and Association Measures”, *Scandinavian Journal of Statistics* **38**(4), 766–780.
- Wood, S. N. (2006), *Generalized Additive Models: An Introduction with R*, Chapman & Hall/CRC.
- Wood, S. N. (2013a), “A Simple Test for Random Effects in Regression Models”, *Biometrika* **100**(4), 1005–1010.
- Wood, S. N. (2013b), “On P-values for Smooth Components of an Extended Generalized Additive Model”, *Biometrika* **100**(1), 221–228.